ATOMISTIC SUMULATIONS OF INTERSECTION CROSS-SLIP NUCLEATION IN Ll$_2$ Ni$_3$Al (Preprint)

D.M. Dimiduk, M.D. Uchic, and C. Woodward

Metals Branch
Metals, Ceramics, & NDE Division

S.I. Rao and T.A. Parthasarathy

UES Inc.

NOVEMBER 2011

STINFO COPY

AIR FORCE RESEARCH LABORATORY
MATERIALS AND MANUFACTURING DIRECTORATE
WRIGHT-PATTERSON AIR FORCE BASE, OH 45433-7750
AIR FORCE MATERIEL COMMAND
UNITED STATES AIR FORCE

REPORT DOCUMENTATION PAGE

1. REPORT DATE *(DD-MM-YY)*	2. REPORT TYPE	3. DATES COVERED *(From - To)*
November 2011	Journal Article Preprint	01 October 2011 – 01 October 2011

4. TITLE AND SUBTITLE	5a. CONTRACT NUMBER
ATOMISTIC SUMULATIONS OF INTERSECTION CROSS-SLIP NUCLEATION IN Ll$_2$ Ni$_3$Al (Preprint)	IN-HOUSE
	5b. GRANT NUMBER
	5c. PROGRAM ELEMENT NUMBER 62102F

6. AUTHOR(S)	5d. PROJECT NUMBER
D.M. Dimiduk, M.D. Uchic, and C. Woodward (Metals, Ceramics, & NDE Division, Metals Branch)	4347
	5e. TASK NUMBER 20
S.I. Rao and T.A. Parthasarathy (UES Inc.)	**5f. WORK UNIT NUMBER** LM121100

7. PERFORMING ORGANIZATION NAME(S) AND ADDRESS(ES)		8. PERFORMING ORGANIZATION REPORT NUMBER
Metals, Ceramics, & NDE Division, Metals Branch (AFRL/RXLM) Air Force Research Laboratory Materials and Manufacturing Directorate Wright-Patterson Air Force Base, OH 45433-7750 Air Force Materiel Command, United States Air Force	UES Inc.	AFRL-RX-WP-TP-2011-4394

9. SPONSORING/MONITORING AGENCY NAME(S) AND ADDRESS(ES)	10. SPONSORING/MONITORING AGENCY ACRONYM(S)
Air Force Research Laboratory Materials and Manufacturing Directorate Wright-Patterson Air Force Base, OH 45433-7750 Air Force Materiel Command United States Air Force	AFRL/RXLM
	11. SPONSORING/MONITORING AGENCY REPORT NUMBER(S) AFRL-RX-WP-TP-2011-4394

12. DISTRIBUTION/AVAILABILITY STATEMENT
Approved for public release; distribution unlimited.

13. SUPPLEMENTARY NOTES
PAO case number 88ABW-2011-5291, cleared 04 October 2011. The U.S. Government is joint author of this work and has the right to use, modify, reproduce, release, perform, display, or disclose the work. Submitted to Scripta Materialia. Document contains color.

14. ABSTRACT
Using atomistic (molecular statics) simulations with embedded atom potentials, we evaluate the activation barrier for a dislocation to form the PPV lock intersecting a forest dislocation in Ll$_2$ Ni$_3$Al as a function of the superpartial core width. The activation energies were obtained by determining equilibrium configurations (energies) when variable pure tensile or compressive stresses are applied along the [111] direction on the partially cross-slipped state. We show that the PPV lock is stable at the intersection, unlike bulk and that the activation energy for cross-slip at the forest dislocation intersection is significantly lower than that for cross slip in bulk [energy of two separate constrictions]. These results suggest that cross-slip should be preferentially observed at selected screw dislocation intersections in Ll$_2$ Ni$_3$Al.

15. SUBJECT TERMS
Ll$_2$ Ni$_3$Al, atomistic simulations, cross-slip, activation energy, dislocation intersection

16. SECURITY CLASSIFICATION OF:			17. LIMITATION OF ABSTRACT:	18. NUMBER OF PAGES	19a. NAME OF RESPONSIBLE PERSON (Monitor)
a. REPORT Unclassified	**b. ABSTRACT** Unclassified	**c. THIS PAGE** Unclassified	SAR	24	Andrew Rosenberger
					19b. TELEPHONE NUMBER *(Include Area Code)* N/A

Atomistic Simulations of Intersection Cross-Slip Nucleation in L1$_2$ Ni$_3$Al

S.I. Rao*, D.M. Dimiduk, T.A. Parthasarathy*, M.D. Uchic
and C. Woodward

Air Force Research Laboratory, Materials and Manufacturing Directorate,
AFRL/MLLM Wright-Patterson AFB, OH 45433-7817, USA

*UES, Inc., 4401 Dayton-Xenia Rd, Dayton, OH 45432-1894, USA

Abstract

Using atomistic (molecular statics) simulations with embedded atom potentials, we evaluate the activation barrier for a dislocation to form the PPV lock intersecting a forest dislocation in L1$_2$ Ni$_3$Al as a function of the superpartial core width.   The activation energies were obtained by determining equilibrium configurations (energies) when variable pure tensile or compressive stresses are applied along the [111] direction on the partially cross-slipped state.   We show that the PPV lock is stable at the intersection, unlike bulk and that the activation energy for cross-slip at the forest dislocation intersection is significantly lower than that for cross slip in bulk [energy of two separate constrictions].   These results suggest that cross-slip should be preferentially observed at selected screw dislocation intersections in L1$_2$ Ni$_3$Al.

Keywords: L1$_2$ Ni$_3$Al; atomistic simulations, cross-slip; activation energy; dislocation intersection

L1$_2$ Ni$_3$Al shows an anomalous increase in flow stress with temperature. Several theories exist for the yield stress anomaly and all of them rely on the fundamental mechanism of the immobilization of the screw superdislocation by cross-slip. The fundamental mechanism of the locking process of the screw superdislocation as

1

suggested by Paidar et.al by cross-slip (termed the 'PPV' lock) continues to be the building block of many models [1-12]. However, previous atomistic simulations of bulk cross-slip in $L1_2$ Ni_3Al using the Voter potential showed that the PPV lock is stable in the bulk only under very high applied stresses (since the cross-slipped PPV superpartial core is higher in energy compared to the planar core because of elastic interactions) and that the activation energy for cross-slip in the bulk is very high ($> 3eV$) [13]. Recent atomistic simulations determining the activation energy for screw dislocation cross-slip at selected forest dislocation intersections in FCC Nickel (Ni) and Copper (Cu) revealed that the activation energy for cross-slip nucleation at forest dislocation intersections is significantly lower (factor of $3 - 20$) than that in bulk, suggesting that cross-slip should preferentially occur at forest dislocation intersections in FCC Ni and Cu [14-16] . In this study, we interrogate the possibility of screw superdislocation cross-slip nucleation in $L1_2$ Ni_3Al to form the 'PPV' lock at a 120° forest dislocation intersection using three different EAM potentials, Moody, Mishin1 and Mishin2 [17-19], which give varying superpartial core widths for the screw superdislocation. The questions to be answered include : a) Are the PPV locks stable at the forest dislocation intersection and b) what is the activation energy for cross-slip nucleation at the forest dislocation intersection as a function of the screw superdislocation superpartial core width?

The atomistic simulations described here employed the 3-dimensional (3d) parallel molecular dynamics code, LAMMPS [20], developed at Sandia National Laboratory. Initially, 2D simulations with periodic boundary conditions along the x or dislocation line direction ($a<110>$) were performed to determine the APB splitting width of the screw and 120° superdislocation. The x-axis was oriented along $[1\bar{1}0]$, y-axis along $[11\bar{2}]$ and the

z-axis along [111]. The dimensions of the simulation cell were one periodic unit ($a<110>$) along the x-axis and 31.5 nm along both the y- and z- axes. The superdislocations were initially introduced into the 2D simulation cell using their anisotropic elasticity displacement field. Fixed boundary conditions were employed along the y and z axes. Energy minimization was performed using the conjugate gradient technique.

A schematic of the simulation cell used in the 3D atomistic simulations is given in Figure 1 of reference [14]. The 3D simulation cell is a rectangular parallelepiped with the x-axis oriented along [$1\bar{1}0$], y-axis along [$11\bar{2}$] and the z-axis along [111]. The dimensions of the simulation cell are 62.0 nm along the x-axis and 31.5 nm along both the y- and z- axes corresponding to a simulation cell of 5,405,160 atoms. Two $1/2[1\bar{1}0]$ screw-character superpartials, spaced by the APB splitting width along the y direction determined from 2D simulations, are inserted in the middle of the simulation cell using their anisotropic elastic displacement field. Similarly two 120° superdislocations having a Burger's vector of [$\bar{1}01$] and line directions $<0\bar{1}\,\bar{1}>$ spaced 30.0 nm apart (at x = -15.0 and 15.0 nm), were also introduced into the simulation cell using their anisotropic elastic displacement fields. Each of the 120° superdislocations are inserted as two ½[$\bar{1}01$] superpartials, separated by their APB splitting width. The relative positions of the screw and 120° superdislocations are varied to obtain several different core structures for the screw dislocation intersection. For simplicity fixed boundary conditions were applied along all three directions and energy minimization was performed using the conjugate gradient technique.

The partially cross-slipped core structures obtained for the screw ($[\bar{1}10]$ Burger's vector) – 120° ($[\bar{1}01]$ Burger's vector, $[0\bar{1}\bar{1}]$ Line Direction) intersection were subjected to uniform compressive or tensile stresses applied along the [111] direction [15]. Under such a state of stress, there are no resolved shear stresses acting along the Burger's vector for either the screw or the 120° dislocation. Also, there are no applied Escaig stresses acting on the edge components of the screw dislocation on the (111) glide plane. However, there are Escaig stresses acting on the edge components of the screw dislocation on the cross-slip $(11\bar{1})$ plane as well as the forest dislocation on the $(1\bar{1}1)$ plane. Fixed boundary conditions were applied along all three directions and energy minimization was performed using the conjugate gradient technique. Such results were analyzed to obtain the energy differences between the fully glide plane core structure and the activated structure for this intersection.

The approach used in this work to obtain activation energies for transformation from one core structure to another is as follows [15]. As the stress is varied, the relative magnitudes of Escaig stresses on the glide plane and cross-slip plane is changed, thus effecting a variation in the length of the partially cross-slipped region of the screw dislocation. Note that stabilizing each configuration requires manipulation of stresses before, after and at the inflection point in the energy-distance coordinate. By releasing the stress from the stabilized state, the configuration was allowed to "fall" towards either side of the saddle point configuration. This process allowed the identification of the saddle point configuration. Once identified, the absolute energy of this configuration without the applied stress is calculated by freezing a small box of atoms near the core transformation region and relaxed with no stress. This gives an upper bound for the

4

energy of the saddle point. The activation energy is obtained by subtracting the energy of the fully glide plane spread core configuration from that of the saddle point. The only error in this calculation arises from the fact that an arbitrary number of atoms are kept frozen while obtaining the energy of the saddle point configuration without any stress.

The embedded atom potentials used in the simulations are the potentials developed for $L1_2$ Ni_3Al by Angelo, Moody and Baskes [17] based on the Voter and Chen format (Moody) as well as the two $L1_2$ Ni_3Al potentials developed by Mishin et.al. [18,19]. Table 1 gives the lattice parameter, cohesive energy, elastic constants and planar fault energies given by the three $L1_2$ Ni_3Al potentials as well as the Voter potential for $L1_2$ Ni3Al [21] which Parthasarathy et.al. [13] used in their simulations of bulk cross-slip. The three $L1_2$ Ni_3Al potentials used in the simulations give almost identical elastic constants, cohesive energy and lattice parameter close to experiment, whereas the planar fault energies given by the potentials varies significantly. The superpartial core width, d, which is inversely proportional to the effective fault energy $\gamma_{csf} - 0.5\gamma_{111}$, for the screw superdislocation varies from d/b = 2 for potential Mishin2 to d/b = 7 for the Voter potential. The Moody potential gives a d/b ratio of approximately 6 whereas the Mishin1 potential gives a d/b ratio of 4. This allows a determination of cross-slip activation energy at the intersection as a function of the superpartial core width in $L1_2$ Ni_3Al.

In order to illustrate the relaxed screw dislocation geometries we plot the position of atoms with a centrosymmetry parameter significantly different from zero [22]. The centrosymmetery parameter is close to zero in the bulk as well as the {111} and {001} APB regions. They are significantly different from zero at the dislocation core as well as the complex stacking fault region. This allows a depiction of the superpartial core in the

5

relaxed superdislocation geometry. In order to illustrate the cross-slipped-segment products of the screw dislocation the atomic positions are shown in a [111] projection.

Figure 1 gives a plot of high centrosymmetry parameter atoms obtained from 2D simulations, for both the screw and 120° superdislocations, using the three L1$_2$ Ni$_3$Al potentials, Moody, Mishin1 and Mishin2. The plot shows the superpartial cores separated by (111) APB region, for all three potentials. Since the planar fault energies varies from potential to potential, the APB and superpartial core splitting width varies from potential to potential. The superpartial core splitting width for the screw superdislocation obtained with all three potentials are given in Table 1.

Figures 2 and 3 give two different equilibrium partially cross-slipped configurations in the (111) projection obtained from the 3D simulations for the screw dislocation intersection. The Moody potential was used in the simulations in both cases. The two structures were obtained for two different relative positions of the screw and 120° superdislocations. In both cases, the positive screw superpartial is completely on the (111) glide plane whereas the negative screw superpartial, is partially on the (111) glide plane and partially on the (11-1) cross-slip plane. This corresponds to the formation of a PPV lock at the intersection. This result shows that the PPV lock is stable at the screw dislocation intersection, unlike bulk. In Figure 2, the negative superparial forms a constricted node at the intersection whereas in Figure 3, the negative superpartial forms an extended node at the intersection. Similar results were obtained with the other two L1$_2$ Ni$_3$Al potentials, Mishin1 and Mishin2 [18,19]. The structure corresponding to the formation of a partially cross-slipped configuration at the positive superpartial of the screw superdislocation was unstable. This is due to the fact that the cross-slipped

Approved for public release; distribution unlimited.

configuration has a higher energy compared to the planar configuration because of elastic interactions with the negative superpartial, as in bulk and the Escaig stresses acting at the positive superpartial from the intersecting dislocation are not large enough to alter this equilibrium.

Figure 4 gives the activated structure in the (111) projection for the screw superdislocation to cross-slip from the planar configuration to a PPV like configuration at a 120° forest dislocation intersection in L1$_2$ Ni$_3$Al, obtained using the Moody potential. In the activated structure, a small portion of the negative superpartial of the screw supersdislocation is on the (11-1) cross-slip plane near the intersection. This suggests that the activation volume for cross-slip at the intersections with respect to applied Escaig stresses is very low $\sim 10 - 20b^3$. Table 2 gives the activation energy for cross-slip of the screw superdislocation at a 120° forest dislocation intersection in L1$_2$ Ni$_3$Al, obtained using the three potentials, Moody, Mishin1 and Mishin2 [17-19]. Table 2 clearly shows that the activation energy for cross-slip is a strong function of the screw superpartial core width and decreases with decreasing screw superpartial core width. Also, shown in Table 2 is the activation energy for cross-slip of the screw superdislocation in bulk (energy of well separated negative and positive constrictions), estimated using the continuum expression of Bonneville and Escaig [23,24]. Atomistic simulation results for cross-slip nucleation activation energy in bulk Ni$_3$Al, obtained using the Voter potential [21] by Parthasarathy and Dimiduk [13] ~ 2.96 eV, compares favorably with the continuum result, suggesting that the continuum expression of Bonneville and Escaig [23,24] gives a reasonable estimate for the cross-slip nucleation energy in bulk. Table 2 shows that the cross-slip nucleation energy is significantly lower at a 120° forest dislocation intersection

7

as compared to bulk, in L1$_2$ Ni$_3$Al. In addition, the cross-slipped configuration forming a PPV lock becomes stable under no applied stresses at a 120° forest dislocation intersection in L1$_2$ Ni$_3$Al, unlike bulk, where it is stable only under very high applied Escaig stresses [13]. Also, the cross-slip nucleation activation energy for the screw superdislocation at a 120° forest dislocation intersection is is reasonable agreement with experimental estimation of the activation energy from the yield stress anomaly in L1$_2$ Ni$_3$Al [25], whereas the bulk cross-slip activation energy is much too large. All these results suggest that cross-slip should preferentially nucleate at selected forest dislocation intersections in L1$_2$ Ni$_3$Al.

Summarizing, atomistic simulations have been used to determine the cross-slip nucleation activation energy to form a 'PPV' lock at a 120° forest dislocation intersection in L1$_2$ Ni$_3$Al. It is shown that the PPV lock is stable at a 120° forest dislocation intersection, unlike bulk and that the activation energy for cross-slip nucleation at this intersection is significantly lower than that in bulk. Also, the cross-slip nucleation energy is a strong function of the superpartial core width and decreases with decreasing core width. The cross-slip activation energy results at the 120° intersection are in reasonable agreement with experimental estimates from the yield stress anomaly, suggesting that cross-slip should preferentially nucleate at selected screw dislocation intersections in L1$_2$ Ni$_3$Al.

ACKNOWLEDGEMENT

8

REFERENCES

1) Takeuchi S, Kuramoto E, Acta Metall. 1973;21:415.

2) Paidar V, Pope DP, Vitek V, Acta Metall. 1984;32:435.

3) Greenberg BA, Gornostyrev YuN, Yakovenkova LI, Physics Metals Metallogr. 1975;39:52.

4) Greenberg BA, Ivonov MA, Gornostyrev YuN, Karkina LE, Phys.Status Solidi (a) 1976;38:653.

5) Hirsch PB, Phil. Mag. A 1992;65:569.

6) Caillard D, Clement N, Couret A, in Strucutural Intermetallics, edited by R. Darolia et.al. (Warrendale, The Minerals, Metals and Materials Society); 1993:409.

7) Couret A, Caillard D, J.Phys.III 1991;1:885.

8) Hirsch PB, Prog.Mater.Sci. 1992;36:63.

9) Ezz SS, Hirsch PB, Mater.Symp.Proc. 1995;364:35.

10) Saada G, Veyssiere P, in Structural Intermetallics. Edited by R. Darolia et.al. (Warrendale, The Minerals, Metals and Materials Society); 1993:379.

11) Saada G, Veyssiere P, Phil.Mag.A 1992;66:1081.

12) Mills MJ, Chrzan DC, Acta Metall.Mater. 1992;40:3051.

13) Parthasarathy TA, Dimiduk D, Acta Mater. 1996;44:2237.

14) Rao S, Dimiduk DM, El-Awady J, Parthasarathy TA, Uchic MD, Woodward C, Philosophical Magazine2009;89:3351.

15) Rao S, Dimiduk DM, El-Awady J, Parthasarathy TA, Uchic MD, Woodward C, Acta Materialia 2010;58:5547.

16) Rao S, Dimiduk DM, El-Awady J, Parthasarathy TA, Uchic MD, Woodward C, accepted for publication in Acta Materialia 2011.

17) Angelo JE, Moody NR, Baskes MI, Modell.Simul.Mater.Sci.Eng. 1995;3:289.

18) Mishin Y, Acta Materialia 2004;52:1451.

19) Purja Pun GP, Mishin Y, Philosophical Magazine 2009;89:3245.

20) Plimpton SJ, J.Comp.Phys. 1995;117:1.

21) Voter AF, Chen SP, MRS Symp.Proc. 1987;82:175.

22) Kelchner CL, Plimpton SJ, Hamilton JC, Phys.Rev.B 1998;58:11085.

23) Bonneville J, Escaig B, Acta Metall. 1979;27:1477.

24) Rao S, Dimiduk DM, Woodward C, Parthasarathy TA, Phil.Mag.Ltrs. 2011;91:452.

25) Demura M, Golberg D, Hirano T, Intermetallics 2007;15:1322.

Figure Captions:

Figure 1: [111] (X-Y plane)) projection of the core structures obtained from 2D atomistic simulations using the Moody potential for an infinite a) Screw and b) 120° superdislocation in $L1_2$ Ni_3Al. Atoms with centrosymmetry parameter significantly different from zero are shown. The axes dimensions are in units of Angstroms.

Figure 2: [111] (X-Y plane)) projection of one of the partially cross-slipped core structure for a screw-120^0 intersection in $L1_2$ Ni_3Al obtained from atomistic simulations using the Moody potential. Atoms with centrosymmetry parameter significantly different from zero are shown. The axes dimensions are in units of Angstroms. The partially cross-slipped core structure has a constricted node at the intersection.

Figure 3: [111] (X-Y plane)) projection of one of the partially cross-slipped core structure for a screw-120^0 intersection in $L1_2$ Ni_3Al obtained from atomistic simulations using the Moody potential. Atoms with centrosymmetry parameter significantly different from zero are shown. The axes dimensions are in units of Angstroms. The partially cross-slipped core structure has an extended node at the intersection.
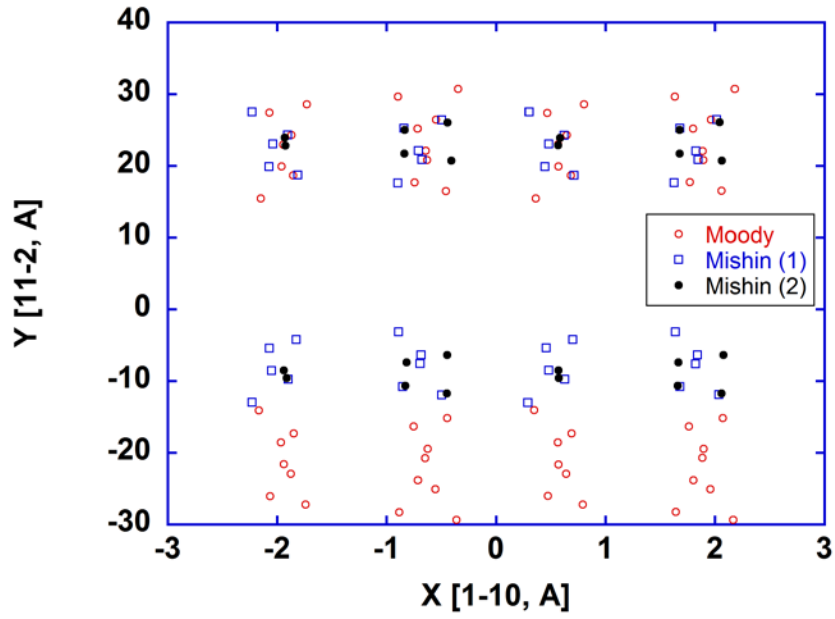
Figure 4: The [111] projection of the structure of the activated configuration for transfer of screw superdislocation from the planar configuration to the partially cross-slipped configuration obtained using the Moody EAM potential for $L1_2$ Ni_3Al. Atoms with centrosymmetry parameter significantly different from zero are shown. The axes dimensions are in units of Angstroms.

11

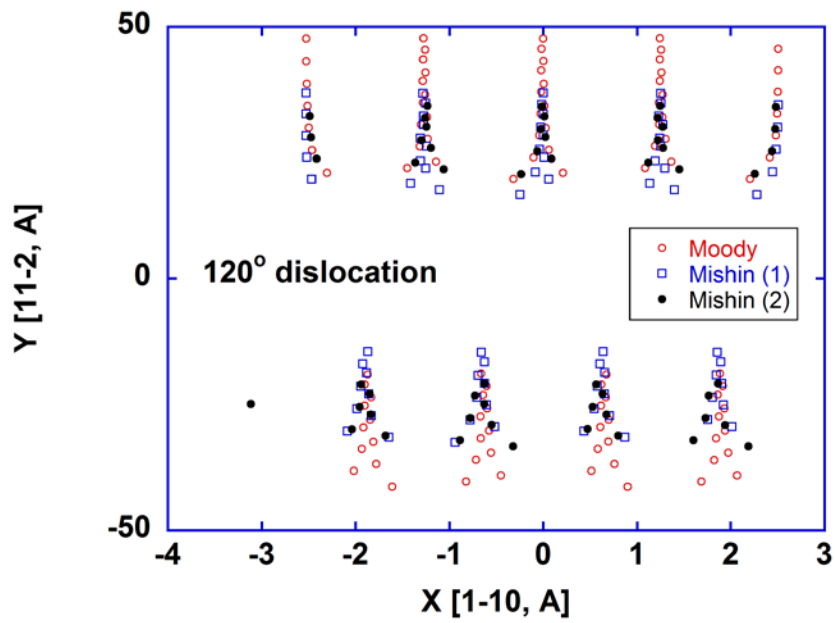|	**Moody**	**Mishin1**	**Mishin2**	**Voter**
a_0, A	3.567	3.571	3.533	3.567
E_c, eV	4.598	4.626	4.632	4.600
C_{11} (x 10^{11} N/m^2)	2.558	2.360	2.382	2.460
C_{12} (x 10^{11} N/m^2)	1.352	1.490	1.664	1.370
C_{44} (x 10^{11} N/m^2)	1.242	1.271	1.302	1.230
γ_{111} (mJ/m^2)	202	252	180	142
γ_{001} (mJ/m^2)	129	80	20	83
γ_{csf} (mJ/m^2)	164	202	228	121
γ_{sisf} (mJ/m^2)	5	51	21	13
γ_{csf} -0.5γ_{111} (mJ/m^2)	63	76	138	50
d/b	6	4	2	7

Table 1: Lattice Parameter, a_o, Cohesive energy, E_c, Elastic constants C_{11}, C_{12} and C_{44}, Planar Fault energies, γ_{111}, γ_{001}, γ_{csf}, γ_{sisf}, γ_{csf}-0.5γ_{111} and the screw superdislocation superpartial core widths, d/b, given by four different EAM potentials for L1$_2$ Ni$_3$Al, Moody, Mishin1, Mishin2 and Voter.

	Moody	**Mishin1**	**Mishin2**	**Voter**
Intersection (eV)	0.90	0.20	< 0.2	-
Bulk (eV)	2.49	0.96	0.15	2.94
d/b	6	4	2	7

Table 2: Activation energy for screw superdislocation cross-slip nucleation to form the 'PPV' lock at a 120° intersection in $L1_2$ Ni3Al obtained using three different EAM potentials, Moody, Mishin1 and Mishin2. Also given are the screw dislocation superepartial core widths, d/b, predicted by the three potentials. Estimates of the cross-slip activation energy in bulk predicted by the three potentials as well as the Voter potential using the Bonneville and Escaig continuum expression are also given.
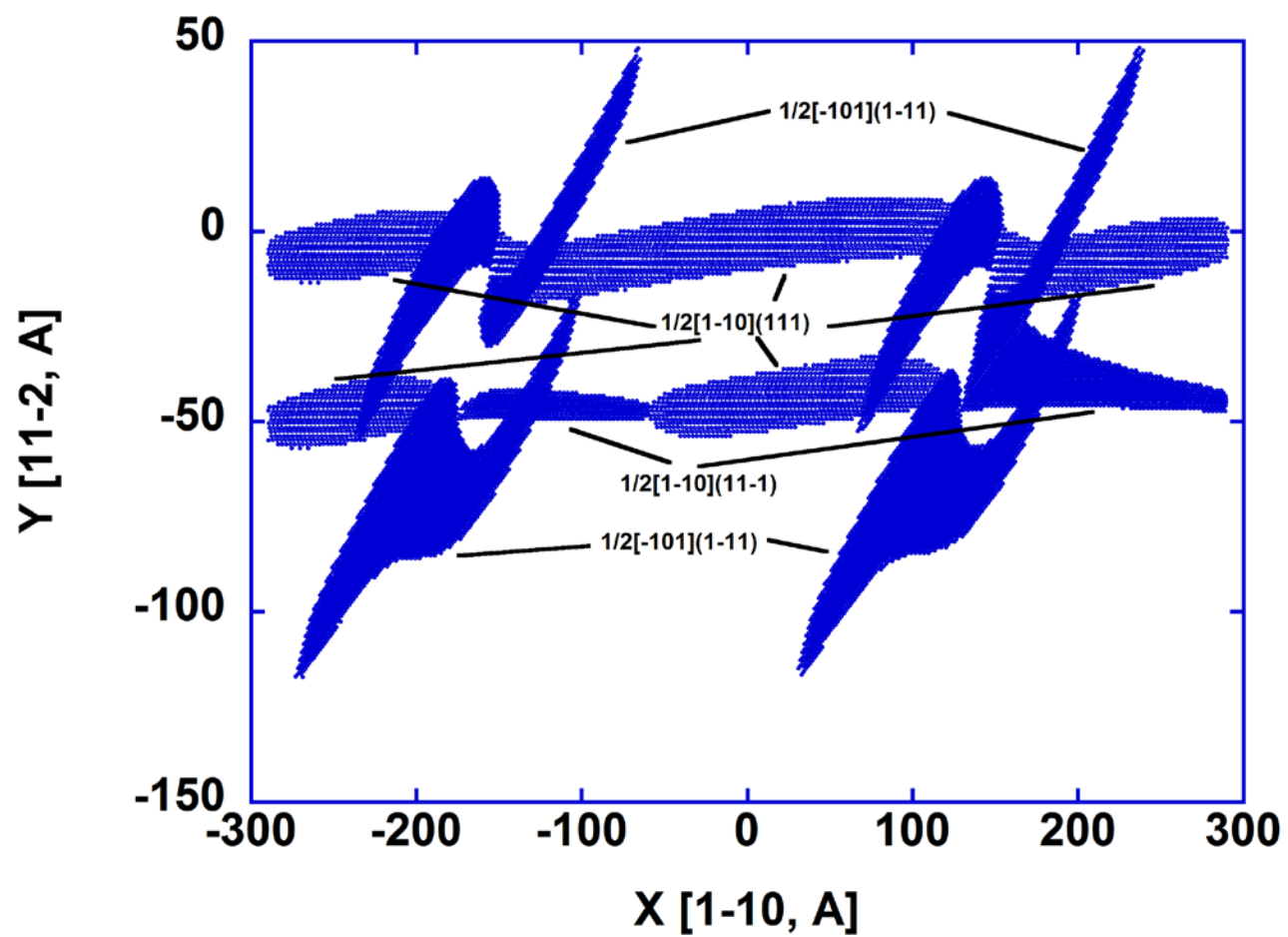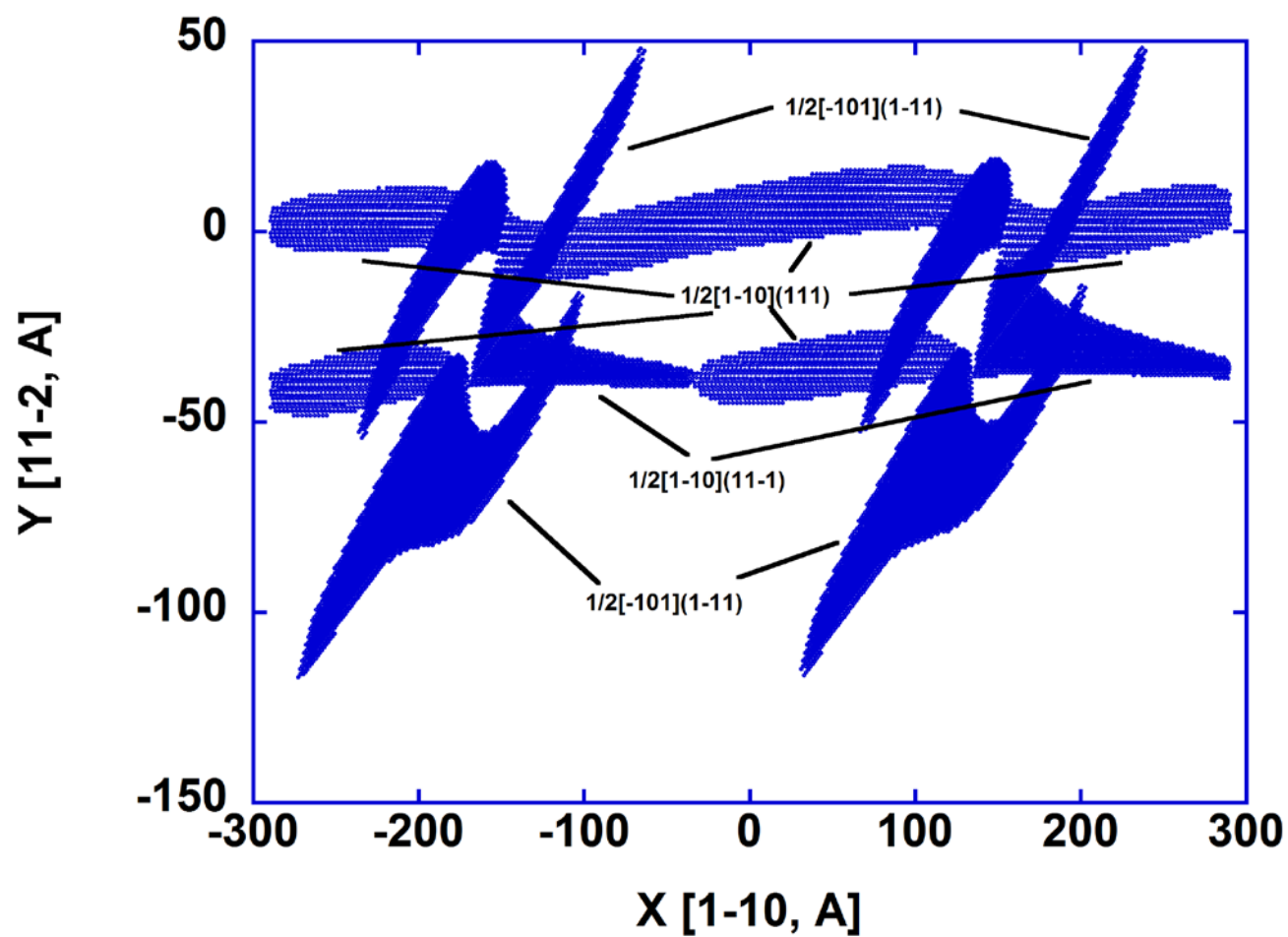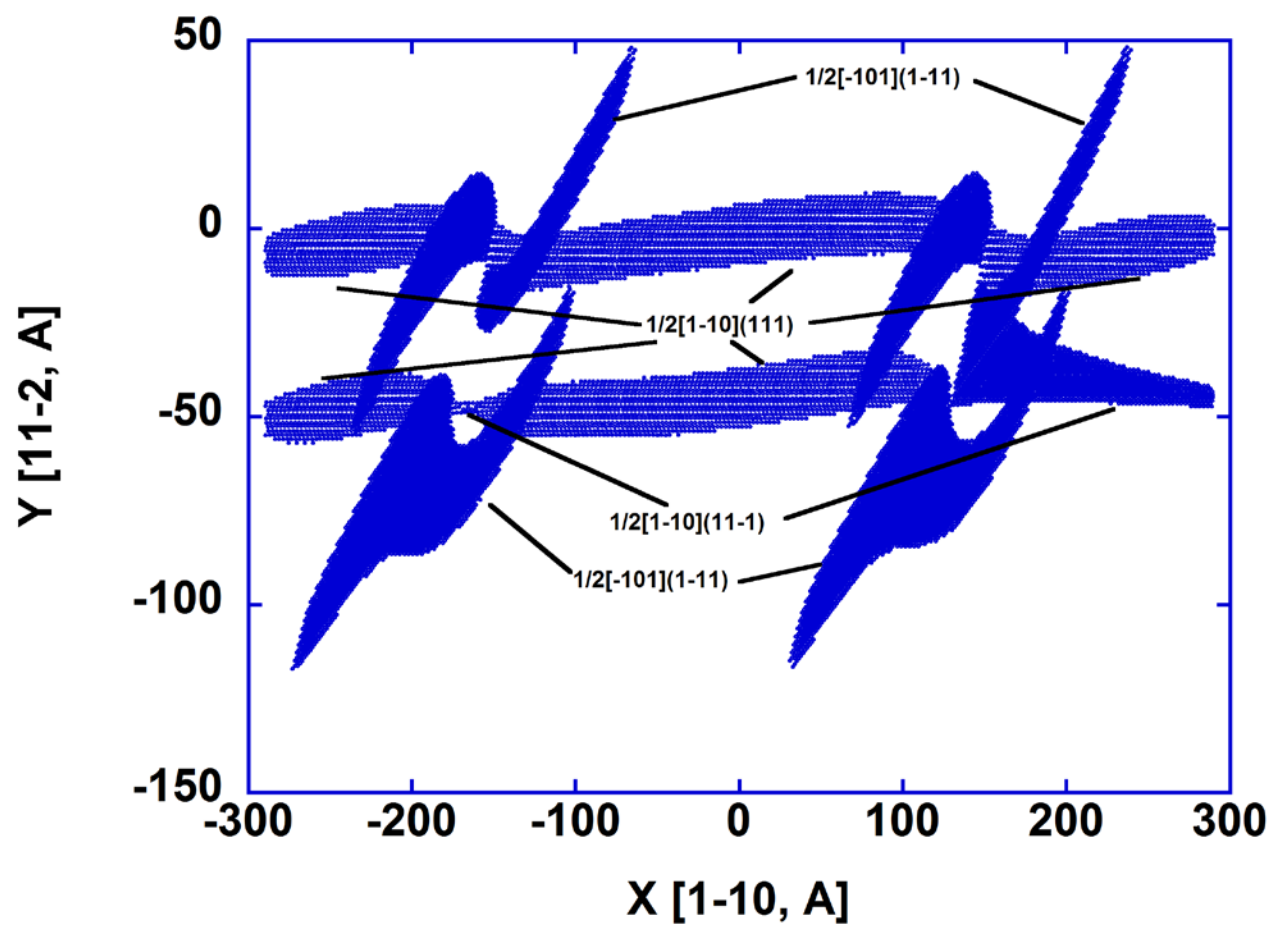
(a)

(b)

Fig.1 :

Fig. 2:

Fig. 3:

Fig.4 :